Current Science International
Volume: 11 | Issue: 02| April - June| 2022

EISSN:2706-7920 ISSN: 2077-4435
DOI: 10.36632/csi/2022.11.2.15
Journal homepage: www.curresweb.com
Pages: 199-216

The stress and strain components for a weakened elastic plate by two curvilinear holes in presence of heat

M. A. Abdou [1], E. Ibrahim[2] and M. Basseem[3]

[1]Department of Mathematics, Faculty of Education, Alexandria University, Egypt.
E-mail: Abdella_777@yahoo.com
[2]Department of Mathematics, Faculty of Science, Helwan University, Egypt.
E-mail: emanebraheem84@yahoo.com
[3]Department of Mathematics, Faculty of Engineering, Sinai University, Egypt.
E-mail: basseem777@yahoo.com.

Received: 15 April 2022 **Accepted:** 20 May 2022 **Published:** 30 May 2022

ABSTRACT
In this work, the first and second Gaursat functions for an unbounded plate with two curvilinear holes are deduced using the complex variable technique. The two holes in all previous works are conformally mapped outside the unit circle. In the presence of an initial heat flow perpendicular to the plate, these are conformally mapped into the unit circle. The holes take on a variety of shapes, allowing this study to be applied to a wide range of situations, including caves, tunnels, and excavations in solids or rocks. The physical meaning of stress components is investigated by obtaining and plotting them. The various forms are received using Maple 2019. There are several applications that are studied and discussed.

Keywords: Thermoelastic plate, Analytical modeling, curvilinear hole, Complex variable method, boundary value problems (BVPs), Gaursat functions, Conformal mapping.

1. Introduction

The complex plane plays a significant role in illustrating some mysteries phenomena like electricity, heat, and magnetic field. Also, it solves many problems in mathematics that can't be in real plane.

Muskhelishvili, (1953) was first who use and developed the method of complex function theory. Some ideas were demonstrated in books, see (Spiegel, 1964; Rubenfeld, 1985; Bieberbach, 1953). Problems with isotropic homogenous cribriform unlimited plate have been investigated in (Muskhelishvili, 1953; Sharma, 2014; Abdou & Khamis, 2000; Abdou & Khar-Eldin, 1994; Colton & Kress, 1983; Abdou, 2003).

Consider a unformal heat $\Theta = qy$ in the negative y- direction, assuming the increasing of temperature Θ is constant throughout the plate's thickness i.e. $\Theta = \Theta(x, y)$, and the temperature gradient is

Corresponding Author: M. A. Abdou, Department of Mathematics, Faculty of Education, Alexandria University, Egypt.E-mail: Abdella_777@yahoo.com

constant. Because of an insulated curvilinear hole C, heat is distributed uniformly, therefore the heat equation must obey the equations. $\nabla^2\Theta = 0, \nabla^2 = \frac{\partial^2}{\partial x^2} + \frac{\partial^2}{\partial y^2}$, ……………………………….(1.1)

$$\frac{\partial\Theta}{\partial n} = 0, r = r_o. \quad \text{……………………………………………………………………………(1.2)}$$

Where n is the normal unit vector of the surface.

The plane theory of elasticity's main problems is just like finding two analytic functions. $\phi(z)$ and $\psi(z)$ of one complex argument $z = x + iy$, these functions, for a point t on the boundary, satisfy the boundary conditions

$$K\,\phi_1(t) - t\,\overline{\phi_1'(t)} - \overline{\psi_1(t)} = f\,(t). \quad \text{……………………………………………………………..(1.3)}$$

If $K = -1$ and $f\,(t)$ is a given function of stress, it is called the first fundamental **BVPs** (the stress **BVPs)**. Putting $K = \chi = \frac{\lambda + 3\mu}{\lambda + \mu}, \lambda = \frac{E}{(1-2\nu)(1+\nu)}$, K is called the thermal conductivity and $f\,(t)$ is a given function of displacement, we have the second fundamental **BVPs** (the displacement **BVPs**).

The complex potential analytic functions $\phi_1(t)$ and $\psi_1(t)$ are:

$$\phi_1(\zeta) = -\frac{S_x + iS_y}{2\pi(1+\chi)}\ln\zeta + c\Gamma\zeta + \varphi(\zeta), \quad \text{…………………………………………………..…(1.4)}$$

and

$$\psi_1(\zeta) = \chi\frac{(S_x - iS_y)}{2\pi(1+\chi)}\ln\zeta + c\Gamma^*\zeta + \psi(\zeta). \quad \text{………………………………………………..(1.5)}$$

Here, S_x , *and* S_y are the vector components of all outer forces acting on the boundary's resulting vector components; Γ , *and* Γ^* are complex constants, $\varphi(\infty) = 0, \psi(\infty) = 0.$

The components of stresses are given by, see (Jaha & Abdou, 2011; Abdou & Aseeri, 2009; Bayones & Alharbi, 2015).

$$\sigma_{xx} = 2G\left[\frac{-1}{2}\left(\frac{\partial^2\phi}{\partial y^2} - \frac{\partial^2\phi}{\partial x^2} + 2\lambda\Theta\right) + \text{Re}[2\phi'(z) - M\,(z, \bar{z})]\right], \quad \text{………………………………..(1.6)}$$

$$\sigma_{yy} = 2G\left[\frac{1}{2}\left(\frac{\partial^2\phi}{\partial y^2} - \frac{\partial^2\phi}{\partial x^2} - 2\lambda\Theta\right) + \text{Re}[2\phi'(z) + M\,(z, \bar{z})]\right], \quad \text{……………………………..…(1.7)}$$

and,

$$\sigma_{xy} = 2G\left[\frac{\partial^2 \phi}{\partial x \partial y} + \text{Im}\{M(z,\bar{z})\}\right],$$

……………………………………………………………...(1.8)

where, $M(z,\bar{z}) = \bar{z}\phi''(z) + \psi'(z)$.

The rational mapping

$$z = c\omega(\zeta) = c\,\frac{\zeta + m_1\zeta^{-1} + m_2\zeta^{-2}}{(1-n_1\zeta^{-1})(1-n_2\zeta^{-1})}, c > 0\,, n_1 \neq n_2 \quad \text{……………………………………….(1.9)}$$

where $z'(\zeta)$ does not vanish or become infinite inside the unit circle γ, has been used.

Here, we will map the boundary of the given C region bounded by the middle plane of the plate in the $z-$plane ($z = x + iy$), by using the same rational mapping but the origin lies inside the hole.

Hence, the conformal mapping used will be modified as

$$z = c\omega(\zeta) = c\,\frac{\zeta^{-1} + m_1\zeta + m_2\zeta^2}{(1-n_1\zeta)(1-n_2\zeta)}, (c > 0\,, n_1 \neq n_2, (|n_1\zeta|;|n_2\zeta| < 1). \text{…………………………...(1.10)}$$

Where, m_1, m_2, n_1, n_2 are real parameters,

2. Rational mapping

Here, we will compare between the shapes of hole in the following cases

I. $n_1\, or\, n_2 = 0, m_1, m_2 \neq 0.$

Here, the conformal mapping $z = c\,\dfrac{\zeta^{-1} + m_1\zeta + m_2\zeta^2}{1 - n\zeta}.$

II. $m_1 = 0, n_1, n_2, m_2 \neq 0, n_1 \neq n_2.$

Here, the conformal mapping $z = c\,\dfrac{\zeta^{-1} + m_2\zeta^2}{(1-n_1\zeta)(1-n_2\zeta)}.$

III. $m_2 = 0, n_1, n_2, m_1 \neq 0, n_1 \neq n_2.$

Here, the conformal mapping $z = c\,\dfrac{\zeta^{-1} + m_1\zeta}{(1-n_1\zeta)(1-n_2\zeta)}.$

IV. $n_1 = n_2 \neq 0, m_1, m_2 \neq 0.$

Here, the conformal mapping $z = c\,\dfrac{\zeta^{-1} + m_1\zeta + m_2\zeta^2}{(1-n\zeta)^2}.$

We used the same numbers in all cases, to find how the condition effects on each case.

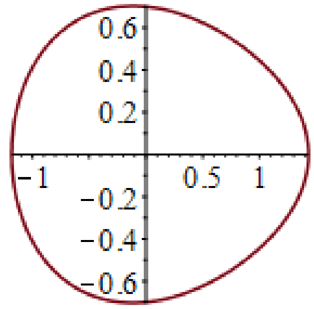

Fig. (2.1).
$n_1=0.03,\ n_2=0.05, m_1=0.3, m_2=0.02.$

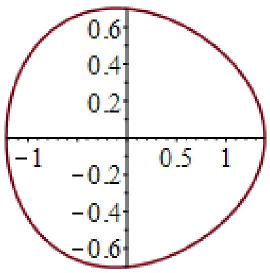

Fig. (2.1.1).
$n_1=0,\ n_2=0.05, m_1=0.3, m_2=0.02.$

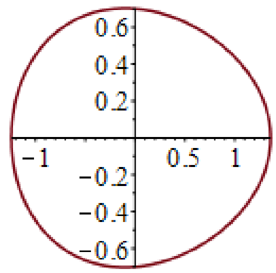

Fig. (2.1.2).
$n_1=0.03,\ n_2=0, m_1=0.3, m_2=0.02.$

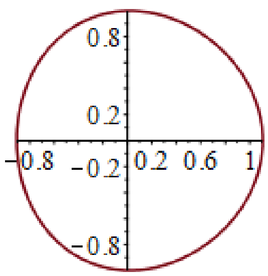

Fig. (2.1.3).
$n_1=0.03,\ n_2=0.05, m_1=0, m_2=0.02.$

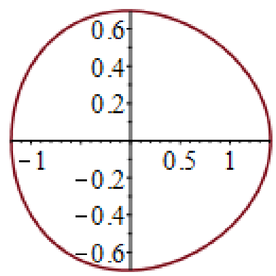

Fig. (2.1.4).
$n_1=0.03,\ n_2=0.05, m_1=0.3, m_2=0.$

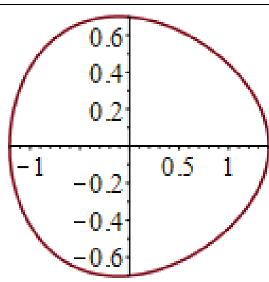

Fig. (2.1.5).
$n_1=n_2=0.03, m_1=0.3, m_2=0.02.$

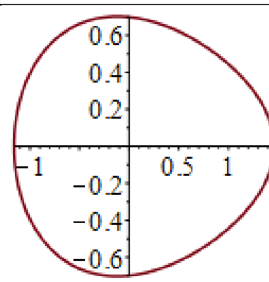

Fig. (2.1.6).
$n_1=n_2=0.05, m_1=0.3, m_2=0.02.$

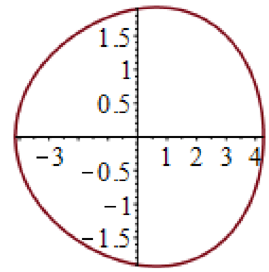

Fig. (2.2).
n_1=0.1, n_2=-0.2,m_1=3,m_2=0.5.

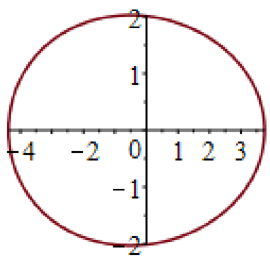

Fig. (2.2.1).
n_1=0, n_2=-0.2,m_1=3,m_2=0.5.

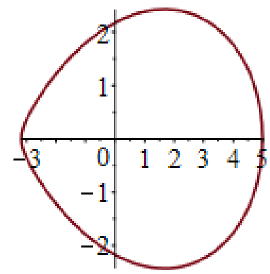

Fig. (2.2.2).
n_1=0.1, n_2=0,m_1=3,m_2=0.5.

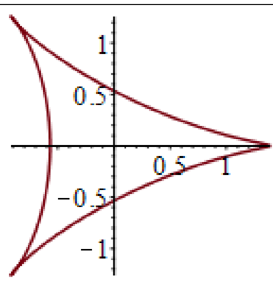

Fig. (2.2.3).
n_1=0.1, n_2=-0.2,m_1=0,m_2=0.5.

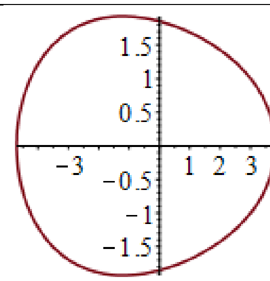

Fig. (2.2.4).
n_1=0.1, n_2=-0.2,m_1=3,m_2=0.

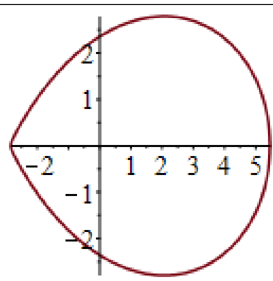

Fig. (2.2.5).
$n_1 = n_2 = 0.1$,m_1=3,m_2=0.5.

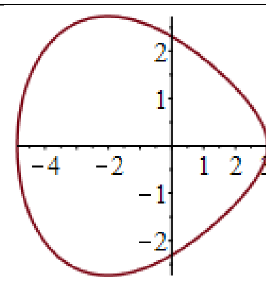

Fig. (2.2.5).
$n_1 = n_2 = -0.2$,m_1=3,m_2=0.5.

Curr. Sci. Int., 11(2): 199-216, 2022
EISSN: 2706-7920 ISSN: 2077-4435 **DOI: 10.36632/csi/2022.11.2.15**

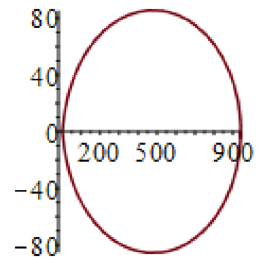

Fig. (2.3)
n_1=0.9, n_2=0.4,m_1=-5,m_2=0.5.

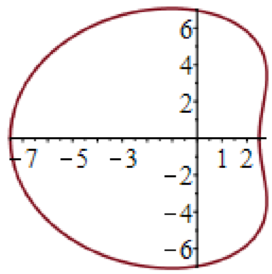

Fig. (2.3.1)
n_1=0, n_2=0.4,m_1=-5,m_2=0.5.

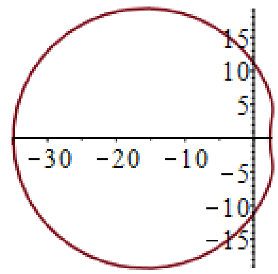

Fig. (2.3.2)
n_1=0.9, n_2=0,m_1=-5,m_2=0.5.

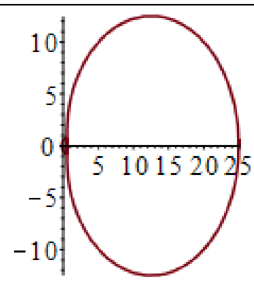

Fig. (2.3.3)
n_1=0.9, n_2=0.4,m_1=0,m_2=0.5.

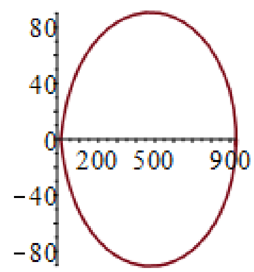

Fig. (2.3.4)
n_1=0.9, n_2=0.4,m_1=-5,m_2=0.

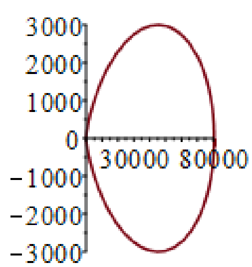

Fig. (2.3.5)
n_1=n_2=0.9,m_1=-5,m_2=0.5.

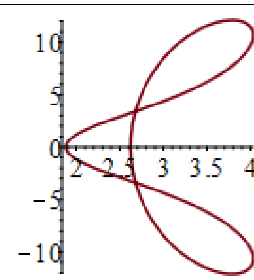

Fig. (2.3.6)
n_1=n_2=0.4,m_1=-5,m_2=0.5.

EISSN: 2706-7920 ISSN: 2077-4435 **DOI: 10.36632/csi/2022.11.2.15**

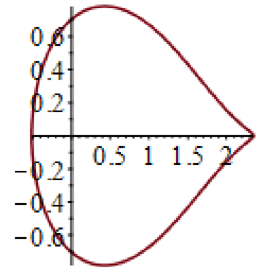

Fig. (2.4)
n_1=0.2, n_2=0.5,m_1=-1,m_2=-0.01.

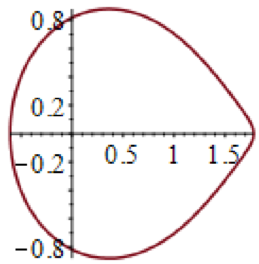

Fig. (2.4.1)
n_1=0, n_2=0.5,m_1=-1,m_2=-0.01.

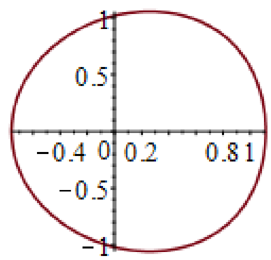

Fig. (2.4.2)
n_1=0.2, n_2=0,m_1=-1,m_2=-0.01.

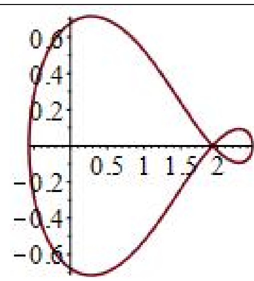

Fig. (2.4.3)
n_1=0.2, n_2=0.5,m_1=0,m_2=-0.01.

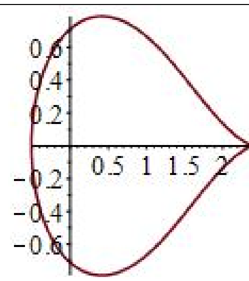

Fig. (2.4.4)
n_1=0.2, n_2=0.5,m_1=-1,m_2=0.

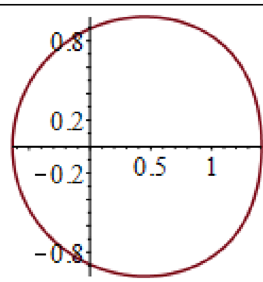

Fig. (2.4.5)
n_1=n_2=0.2,m_1=-1,m_2=-0.01.

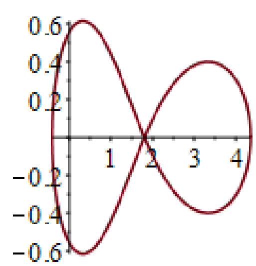

Fig. (2.4.6)
n_1=n_2=0.5,m_1=-1,m_2=-0.01.

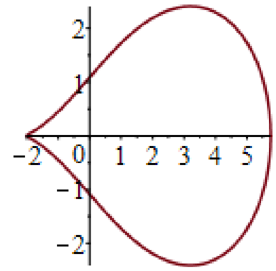

Fig. (2.5)
n_1=0.5, n_2=0.02,m_1=2,m_2=-0.1.

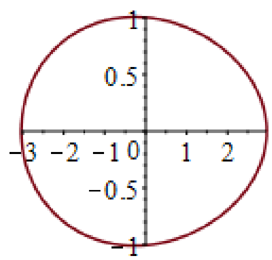

Fig. (2.5.1)
n_1=0, n_2=0.02,m_1=2,m_2=-0.1.

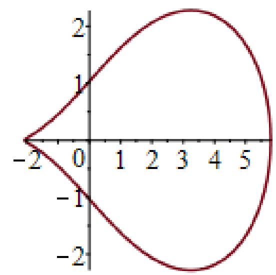

Fig. (2.5.2)
n_1=0.5, n_2=0,m_1=2,m_2=-0.1.

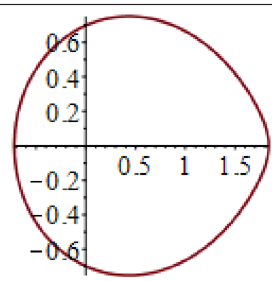

Fig. (2.5.3)
n_1=0.5, n_2=0.02,m_1=0,m_2=-0.1.

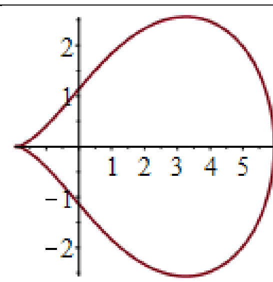

Fig. (2.5.4)
n_1=0.5, n_2=0.02,m_1=2,m_2=0.

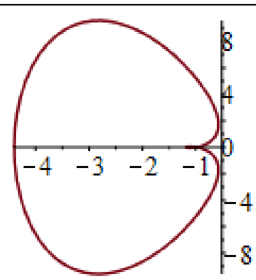

Fig. (2.5.5)
n_1=n_2=0.5,m_1=2,m_2=-0.1.

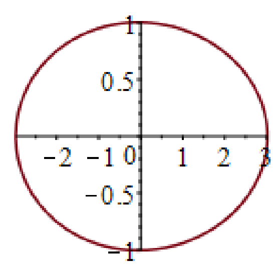

Fig. (2.5.5)
n_1=n_2=0.02,m_1=2,m_2=-0.1.

1. It seems that all figures are similar about $x-axis$.
2. In Fig. (2.1), the general case is when $n_1=0.03, n_2=0.05, m_1=0.3, m_2=0.02$, it is obvious that all the special cases are as same as the original one, except in case of $m_1=0$.
3. In Fig. (2.2), $n_1=0.1, n_2=-0.2, m_1=3, m_2=0.5$, all cases are different from each other. When $n_1=0$, there is enlargement in $y-axis$ only, while when $n_2=0$, the enlargement in both axes. When $m_1=0$, the shape of hole is completely changed, while when $m_2=0$, there is a little reduction in $x-axis$. When $n_1=n_1=0.1$ & $n_1=n_1=-0.2$, the two figures are almost the same but inverse to each other.
4. In Fig. (2.3), the general case is when $n_1=0.9, n_2=0.4, m_1=-5, m_2=0.5,$ in case of $n_1=0$ & $n_2=0$, the shape of holes is changed and there is a big reduction in figs. (2.3.1) - (2.3.2). when $m_2=0$, it is like as same as Fig. (2.3), but when $m_1=0$, there is reduction in area keeping the same shape of general case. When $n_1=n_2=0.9$, a big enlargement in the area of holes occurred, while when $n_1=n_2=0.4$, there is a singularity point.
5. In Fig. (2.4), the general case is when $n_1=0.2, n_2=0.5, m_1=-1, m_2=-0.01$. When $n_1=0$, the shape of hole is somewhat like the original one, while when $n_2=0$, it is completely changed. when $m_1=0$, there is a singularity point, while when $m_2=0$, the shape of hole is identical as the general one. When $n_1=n_2=0.2$,the shape of holes is completely changed, in the other hand when $n_1=n_2=0.5$, there is a singularity point.
6. In Fig. (2.5), the general case is when $n_1=0.5, n_2=0.02, m_1=2, m_2=-0.1$ in case of $n_1=0$ & $n_1=n_2=0.02$, the shape of hole is somewhat like circle, when $n_2=0$ & $m_2=0$, the shape of hole is as same as the general one, when $m_1=0$ & $n_1=n_2=0.5$, the shape of hole is completely changed.
7. The Figs. (2.3.6), (2.4.3) and (2.4.6) have singularity points and this are in valid figures.

3. Gaursat functions (analytic potential complex functions) :

After using the conformal mapping (1.10), we can write the function $\dfrac{\omega(\zeta)}{\omega'(\zeta^{-1})}$ as,

$$\frac{\omega(\zeta)}{\omega'(\zeta^{-1})}=\alpha(\zeta)+\beta(\zeta^{-1}), \quad \text{……………………………………………………………..……..(3.1)}$$

$$\alpha(\zeta)=\frac{h_j n_j}{1-n_j\zeta},$$

$$h_j=\frac{(n_j+m_1n_j^{-1}+m_2n_j^{-2})(1-n_j^2)^2(1-n_1n_2)^2}{(1-n_j^{-1}n_{j\pm1})[m_2n_j(2-n_1n_2-n_j^2)+m_1(1-n_{j\pm1}n_j^3)-n_j^{-2}(1-2n_1n_2)-3n_1n_2]}, j=1,2.$$

…………...……(3.2)

$\beta(\zeta^{-1})$ is a regular function for $|\zeta|<1$.

Hence, the formula (1.1) after using Eqs. (1.2) and (1.3) with the aid of (3.1), yields

$$K\varphi(\sigma)-\alpha(\sigma)\overline{\varphi'(\sigma)}-\overline{\psi_*(\sigma)}=F_*(\sigma)\,, \qquad (3.3)$$

where,

$$\psi_*(\sigma)=\psi(\sigma)+\beta(\sigma)\,\varphi'(\sigma), \qquad (3.4)$$

$$F_*(\sigma)=F(\sigma)-cK\,\Gamma\sigma-c\overline{\Gamma^*}\sigma^{-1}+N(\sigma)[\,\alpha(\sigma)+\overline{\beta(\sigma)}\,], \qquad (3.5)$$

$$N(\sigma)=c\overline{\Gamma}-\frac{S_x-iS_y}{2\pi(1+\chi)}\sigma,\quad F(\sigma)=f\,(c\,\omega(\sigma))=f\,(t). \qquad (3.6)$$

where, the function $F(\sigma)$ and its derivatives satisfy Hölder condition.

To determine $\varphi(\sigma)$, multiply Eq. (2.3) by $\frac{d\sigma}{2\pi i\,(\sigma-\zeta)}$ where ζ is any point lies in the region γ and integrating over the circle, we have

$$K\varphi(\zeta)-\frac{1}{2\pi i}\int_\gamma\frac{\alpha(\sigma)\,\overline{\varphi'(\sigma)}}{(\sigma-\zeta)}d\sigma=\sum_{j=1}^{2}[\frac{h_jn_j}{1-n_j\zeta}N\,(n_j^{-1})-\frac{cK\Gamma}{1-n_j\zeta}]+A(\zeta), \qquad (3.7)$$

where,

$$A(\zeta)=\frac{1}{2\pi i}\int_\gamma\frac{F(\sigma)}{(\sigma-\zeta)}d\sigma \qquad (3.8)$$

The integral terms of Eq. (3.7) is

$$\frac{1}{2\pi i}\int_\gamma\frac{\alpha(\sigma)\,\overline{\varphi'(\sigma)}}{(\sigma-\zeta)}d\sigma=c\sum_{j=1}^{2}\frac{h_jb_j}{1-n_j\zeta}, \qquad (3.9)$$

where b_j, $j=1,2$ are constants in the complex form.

Using Eq. (3.9), Eq. (3.7) will be written as

$$K\varphi(\zeta)=\sum_{j=1}^{2}\{\frac{h_jn_j}{1-n_j\zeta}[cb_j+N\,(n_j^{-1})]-\frac{cK\Gamma}{1-n_j\zeta}\}+A(\zeta). \qquad (3.10)$$

After differentiating Eq. (3.10) with respect to ζ and then from Eq. (3.9), we get

$$cb_j=\frac{KE_j+h_jd_j\overline{E}_j}{K^2-h_j^2d_j^2}, \qquad (3.11)$$

where,

$$d_j=\frac{n_j^2}{(1-n_j^2)^2},E_j=\overline{A'(n_j^{-1})}-\frac{cK\Gamma n_j}{(1-n_j^2)^2}+h_jd_j\overline{N\,(n_j^{-1})};\quad j=1,2. \qquad (3.12)$$

The second Gaursat function $\psi(\zeta)$ can be determined from Eq. (3.4).

4. Some applications

Here, we postulated some different applications for the first and second fundamental **BVPs.** In addition, we represent the stress components by figures in presence ad absence of heat.

EISSN: 2706-7920 ISSN: 2077-4435 **DOI: 10.36632/csi/2022.11.2.15**

Application 1: Unbounded plate with a curved hole under the effect of uniform tensile stress and flux of heat:

Assume $K=-1, \Gamma=\frac{P}{4}; \quad \Gamma^{*}=\frac{-P}{2}e^{-2i\theta}; \quad 0\le\theta\le 2\pi,\ S_x=S_y=f=0.$

Then, the Gaursat functions become

$$\varphi(\zeta)=-c\left[\frac{P/4}{1-n_j\zeta}+\sum_{j=1}^{2}\frac{h_j n_j}{1-n_j\zeta}\left(\frac{P}{4}+b_j\right)\right], \quad \text{(4.1)}$$

$$\psi(\zeta)=-\frac{cP}{4}\left(\zeta^{-1}-\frac{\zeta}{\zeta-n_j}\right)+\frac{cP}{2}e^{-2i\theta}\zeta-\frac{\omega(\zeta^{-1})}{\omega'(\zeta)}\varphi_*(\zeta)+\sum_{j=1}^{2}\frac{h_j n_j\zeta}{\zeta-n_j}\varphi_*(n_j),$$

$$\varphi_*(\zeta)=\varphi'(\zeta)+\frac{cP}{4} \quad \text{(4.2)}$$

The Gaursat functions for an unbounded plate with two curvilinear holes C . The plate will stretch at infinity after applying a uniform tensile stress of intensity P , which makes an angle θ with the $x-$ axis.

For n_1=0.03, n_2=0.05, m_1=0, m_2=0.02, P=0.25,q=0.3, ν=0.25,$\alpha_p=0.7, and\ G=0.5$, the relationship between the stress components $\sigma_{xx}, \sigma_{yy}, \sigma_{xy}$ and the angle θ are shown in Figs. (4.1)-(4.4).

Curr. Sci. Int., 11(2): 199-216, 2022
EISSN: 2706-7920 ISSN: 2077-4435 **DOI: 10.36632/csi/2022.11.2.15**

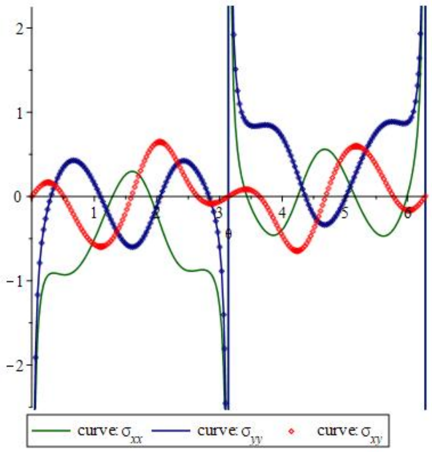

Fig. (4.1). the stress functions in presence of heat Θ according to Application 1.

The maximum value of σ_{xx} is $(2.22, \theta = 3.215 \,\&\, 6.214)$,

The minimum value of σ_{xx} is $(-2.47, \theta = 0.018 \,\&\, 3.071)$,

The maximum value of σ_{yy} is $(2.22, \theta = 3.215 \,\&\, 6.214)$,

The minimum value of σ_{yy} is $(-2.47, \theta = 0.018 \,\&\, 3.071)$,

The maximum value of σ_{xy} is $(0.647, \theta = 2.059)$,

The minimum value of σ_{xy} is $(-0.645, \theta = 1.066 \,\&\, 4.209)$.

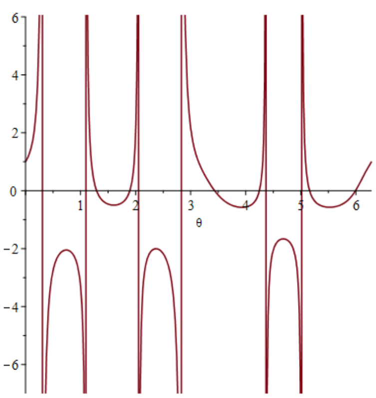

Fig. (4.2). The ratio between the two normal stress in presence of heat Θ according to Application 1.

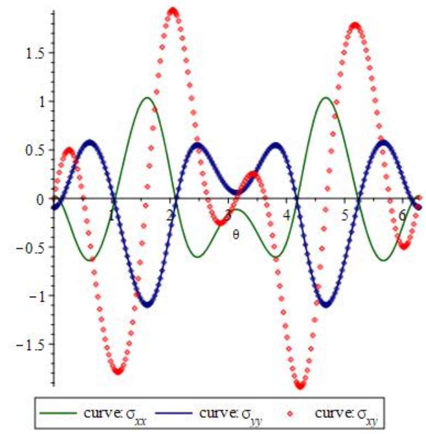

Fig. (4.3). the stress functions in absence of heat Θ according to Application 1.

The maximum value of σ_{xx} is $(1.035, \theta = 1.557 \,\&\, 4.672)$,

The minimum value of σ_{xx} is $(-0.638, \theta = 0.619 \,\&\, 5.648)$,

The maximum value of σ_{yy} is $(0.589, \theta = 0.6 \,\&\, 5.648)$,

The minimum value of σ_{yy} is $(-1.097, \theta = 1.614 \,\&\, 4.672)$,

The maximum value of σ_{xy} is $(1.928, \theta = 2.045)$,

The minimum value of σ_{xy} is $(-1.928, \theta = 4.241)$.

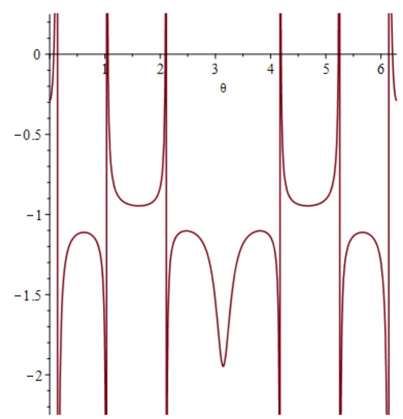

Fig. (4.4). The ratio between the two normal stress in absence of heat Θ according to Application 1.

Application 2: A curved hole with two poles that is subjected to a constant pressure P: If $K = -1$, $S_x = S_y = \Gamma = \Gamma^* = 0$, $f(t) = Pt$, $\Theta = q\,y$. We get

$$\varphi(\zeta) = -c\left[\frac{P}{\zeta} + \sum_{j=1}^{2}\frac{h_j n_j b_j}{1 - n_j \zeta}\right], \quad \ldots\ldots(4.3)$$

$$\psi(\zeta) = cP\zeta - cP(n_1 + n_2) - \frac{\omega(\zeta^{-1})}{\omega'(\zeta)}\varphi'(\zeta) + \sum_{j=1}^{2}\frac{h_j \zeta}{1 - n_j \zeta}\varphi'(n_j). \quad \ldots\ldots(4.4)$$

Thus, Eqs. (4.3)- (4.4) are the first fundamental problem solution for an isotropic unbounded plate with the curvilinear hole, in absence of external force and a uniform pressure P is subjected to edges.

For n_1=0.03, n_2=0.05, m_1=0, m_2=0.02, P=0.25,q=0.3, ν=0.25,$\alpha_p = 0.7, and\ G = 0.5$, the relationship between the stress components $\sigma_{xx}, \sigma_{yy}, \sigma_{xy}$ and the angle θ are shown in Figs. (4.5) - (4.8).

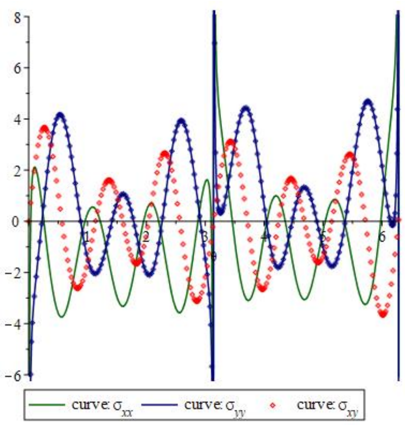

The maximum value of σ_{xx} is $(8, \theta = 3.161 \,\&\, 7.35)$,

The minimum value of σ_{xx} is $(-6, \theta = 0 \,\&\, 3.161)$,

The maximum value of σ_{yy} is $(8, \theta = 3.161 \,\&\, 7.35)$,

The minimum value of σ_{yy} is $(-6, \theta = 0 \,\&\, 3.161)$,

The maximum value of σ_{xy} is $(3.722, \theta = 0.253)$,

The minimum value of σ_{xy} is $(-3.721, \theta = 5.997)$.

Fig. (4.5). the stress functions in presence of heat Θ according to Application 2.

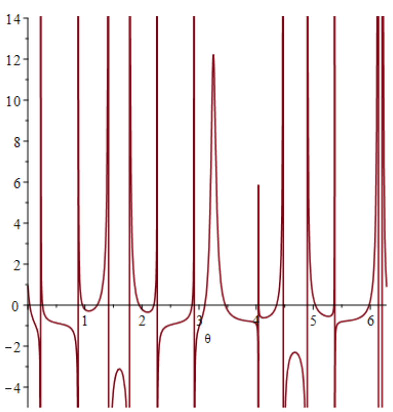

Fig. (4.6). The ratio between the two normal stress in presence of heat Θ according to Application 2.

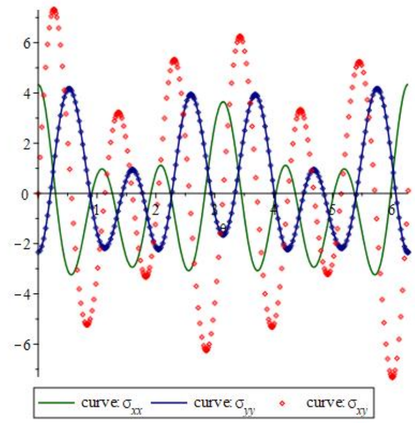

Fig. (4.7). the stress functions in absence of heat Θ according to Application 2.

The maximum value of σ_{xx} is $(4.227, \theta = 0\,\&\,6.25)$,

The minimum value of σ_{xx} is $(-3.2, \theta = 0.56\,\&\,5.69)$,

The maximum value of σ_{yy} is $(4.181, \theta = 0.56\,\&\,5.762)$,

The minimum value of σ_{yy} is $(-2.359, \theta = 0\,\&\,6.268)$,

The maximum value of σ_{xy} is $(7.264, \theta = 0.253)$,

The minimum value of σ_{xy} is $(-7.311, \theta = 5.997)$.

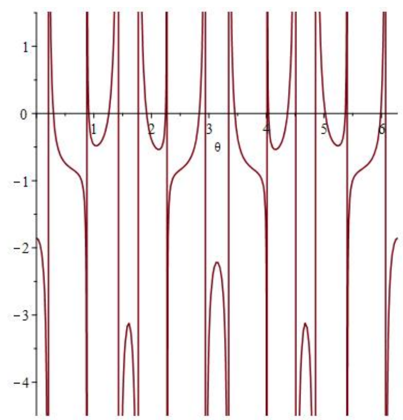

Fig. (4.8). The ratio between the two normal stress in absence of heat Θ according to Application 2.

Application 3: The external force acts on the curvilinear's middle:

When, $k = \chi, \Gamma = \Gamma^* = f = 0$. Then,

$$\chi\varphi(\zeta) = \frac{-c\,\chi P/4}{1-n_j\zeta} + \sum_{j=1}^{2}\frac{h_j n_j}{1-n_j\zeta}\left[N\,(n_j^{-1}) + cb_j\right], \quad \text{...(4.5)}$$

$$\psi(\zeta) = -\frac{\omega(\zeta^{-1})}{\omega'(\zeta)}\varphi_*(\zeta) + \sum_{j=1}^{2}\frac{h_j n_j \zeta}{\zeta - n_j}\varphi_*(n_j^{-1}). \quad \text{...(4.6)}$$

Where, $\varphi_*(\zeta) = \varphi'(\zeta) + \dfrac{cP}{4}$.

When the force acts on the curvilinear kernel, we get the second fundamental boundary problem. The stresses will be assumed to vanish at infinity, and it will be clear that there is no rotation with the kernel.

For n_1=0.03, n_2=0.05, m_1=0, m_2=0.02, P=0.25,q=0.3, ν=0.25, $\alpha_p = 0.7, and\ G = 0.5$, the relationship between the stress components $\sigma_{xx}, \sigma_{yy}, \sigma_{xy}$ and the angle θ are obtained in Figs. (4.9)-(4.12).

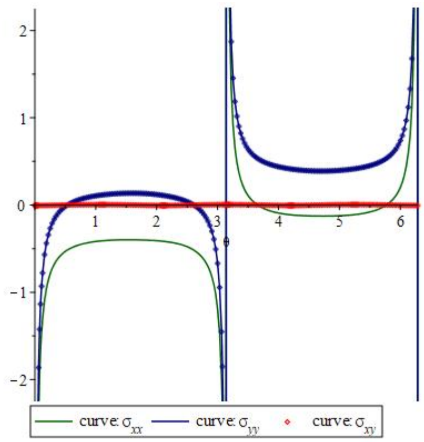

Fig. (4.9). the stress functions in presence of heat Θ according to Application 3.

The maximum value of σ_{xx} is $(20237, \theta = 3.179 \,\&\, 6.195)$,

The minimum value of σ_{xx} is $(-2.212, \theta = 0.055 \,\&\, 3.07)$,

The maximum value of σ_{yy} is $(20237, \theta = 3.179 \,\&\, 6.195)$,

The minimum value of σ_{yy} is $(-2.212, \theta = 0.055 \,\&\, 3.07)$,

σ_{xy} is equal to zero.

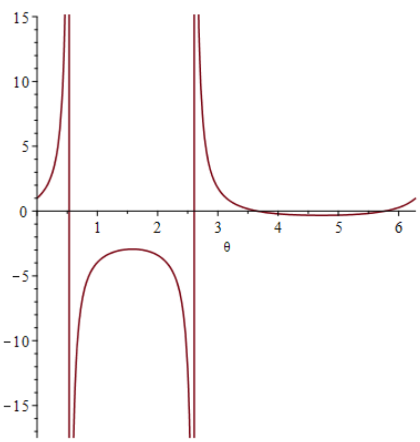

Fig. (4.10). The ratio between the two normal stress in presence of heat Θ according to Application 3.

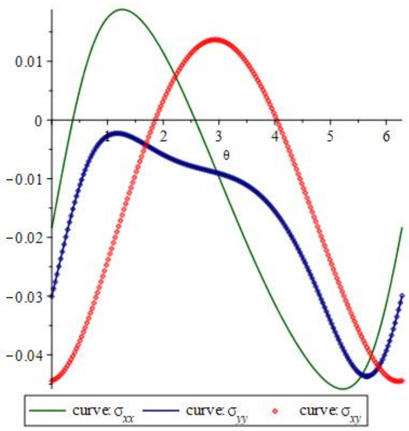

Fig. (4.11). the stress functions in absence of heat Θ according to Application 3.

The maximum value of σ_{xx} is $(0.019, \theta = 1.219)$,

The minimum value of σ_{xx} is $(-0.046, \theta = 5.145)$,

The maximum value of σ_{yy} is $(-0.002, \theta = 1.122)$,

The minimum value of σ_{yy} is $(-0.044, \theta = 5.648)$,

The maximum value of σ_{xy} is $(0.014, \theta = 2.959)$,

The minimum value of σ_{xy} is

$(-0.045, \theta = 0 \,\&\, 6.247)$.

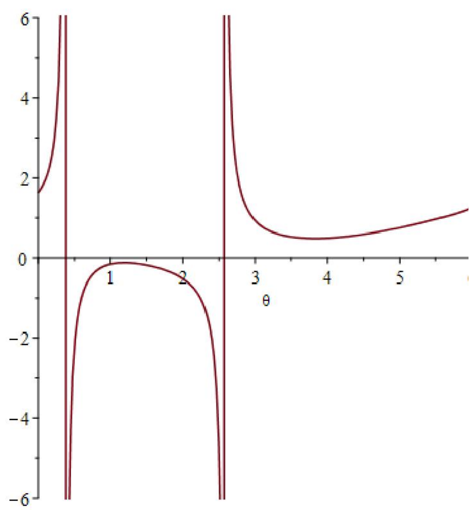

Fig. (4.12). The ratio between the two normal stress in absence of heat Θ according to Application 3.

5. Conclusion

Here, we will show the important points in the previous discussion

(i) Unbounded region was mapped inside the unit circle γ by the conformal mapping $z = c\,\omega(\zeta), c > 0$, where $\omega'(\zeta) \neq 0, \infty$, for $|\zeta| < 1$.

(ii) From boundary value issues, we can obtain the integro-differential equation with discontinuous kernel, when the conformal mapping is applied, $z = c\omega(\zeta), c > 0$.

(iii) In order to solve the integro-differential equation and extract the functions immediately, the Cauchy approach is preferred.

(iv) The components of stress σ_{xx} , σ_{yy} and σ_{xy} can be completely determined, after obtaining the two complex functions.

(v) Positive stress values indicate that stress is in the positive direction, and vice versa, implying that stress operates as a compressive force.

References

Abdou, M. A. and S. Aseeri, 2009. Closed forms of Gaursat functions in presence of heat for curvilinear holes. Journal of thermal stresses, 1126- 1148.

Abdou, M.A. and A.K. Khamis, 2000. On a problem of an infinite plate with a curvilinear hole having three poles and arbitrary shape. Bull. Call. Math. Soc., 29, 104-115

Abdou, M.A., 2003. On Asymptotic Method for Fredholm-Volterra Integral Equation of the Second Kind in Contact Problems. Journal of Computational and Applied Mathematics, **154**, 431-446.

Abdou, M.A., E.A. Khar-Eldin, 1994. An infinite plate weakened by a hole having arbitrary shape. J. Comp. Appl. Math.,Vol. 56, 1994.341-351.

Bayones, F.S. and B.M. Alharbi, 2015. An infinite plate with curvilinear hole having two poles and arbitrary shape in the presence of heat. International journal of scientific and engineering research

Bieberbach, L., 1953. Conformal Mapping. Chelsea Publishing Company, New York.

Colton, D. and R. Kress, 1983. Integral Equation Method in Scattering Theory. John Wiley, New York.

Jaha Y.A. and M.A. Abdou, 2011. Gaursat function for an elastic plate weakened by a curvilinear hole in the presence of heat, International journal of recent research and applied studies, 325-334.

Msukhelishvili, N. I., 1953. Some basic problems of mathematical theory of elasticity. Noordroof, Holladn.

Rubenfeld, L.A., 1985. A First Course in Applied Complex Variables. John Wiley & Sons, New York.

Sharma, D.S., 2014. Moment distribution aroundpolygonal holes in infinite plate. 20 International Journal of Mechanical Sciences, 78(1):177-182.

Spiegel, M.R., 1964. Theory and Problems of Complex Variables, Schaum's Outline Series. McGraw-Hill, New York.